Uniform Convergence Analysis of Finite Difference Scheme for Singularly Perturbed Delay Differential Equation on an Adaptively Generated Grid

Jugal Mohapatra and Srinivasan Natesan[*]

Department of Mathematics, Indian Institute of Technology Guwahati, Guwahati – 781 039, India.

Abstract. Adaptive grid methods are established as valuable computational technique in approximating effectively the solutions of problems with boundary or interior layers. In this paper, we present the analysis of an upwind scheme for singularly perturbed differential-difference equation on a grid which is formed by equidistributing arc-length monitor function. It is shown that the discrete solution obtained converges uniformly with respect to the perturbation parameter. Numerical experiments illustrate in practice the result of convergence proved theoretically.

AMS subject classifications: 65L10, 65L12

Key words: Singular perturbation problems, delay differential equations, boundary layer, upwind scheme, adaptive mesh, uniform convergence.

1. Introduction

In this article, we consider the following singularly perturbed delay differential equation:

$$\begin{cases} \mathscr{L}_\varepsilon u_\varepsilon(x) \equiv -\varepsilon u_\varepsilon''(x) - a(x)u_\varepsilon'(x-\delta) + b(x)u_\varepsilon(x) = f(x), & x \in \Omega = (0,1), \\ u_\varepsilon(x) = \gamma(x), & -\delta \le x \le 0, \\ u_\varepsilon(1) = \lambda, \end{cases} \tag{1.1}$$

where $0 < \varepsilon \ll 1$ is a small parameter and the delay parameter δ is such that $0 < \delta < 1$, which is of $o(\varepsilon)$. The functions $a(x), b(x), f(x)$ and $\gamma(x)$ are sufficiently smooth functions and λ is a constant. It is also assumed that $b(x) \ge \beta > 0, \forall x \in \overline{\Omega}$. Such a problem is sometimes addressed as two-parameter problem. The argument for small delay problems

---

[*]Corresponding author. *Email addresses:* `jugal@iitg.ernet.in` (J. Mohapatra), `natesan@iitg.ernet.in` (S. Natesan)

are widespread in many mathematical models of biophysics and mechanics where delay term plays an important role in modelling real-life phenomena [12].

When $\delta = 0$, the above equation (1.1) reduces to a singularly perturbed differential equation with a single parameter ε. Depending upon the sign of $a(x)$, *i.e.,* if $a(x) > 0$ (or $a(x) < 0$), a boundary layer is located at left (or right) end of the domain. The layer is maintained for sufficiently small δ with $\delta \neq 0$ and $\delta = o(\varepsilon)$. Lange et al. [5,6] provided an asymptotic approach to boundary value problems (BVP) of the type (1.1). By considering several examples, they have shown that the effect of the small delay on the solution cannot be neglected.

The solution of (1.1) has steep layers which are difficult to approximate efficiently by most numerical methods using uniform grid [4]. In this context, one may think of solving the above problem with a suitably chosen non-uniform grid. If the presence, location, and thickness of a boundary layer is known a priori, then highly appropriate non-uniform grids can be generated. The main disadvantage of this kind of approach is that it relies heavily on knowing a considerable amount about the exact solution before one attempts to solve the differential equation.

A more widely applicable idea is to use an adaptive non-uniform grid where adaptivity is governed by the numerical solution. This approach has the advantage that it can be applied using little or no a priori information. The objective of this paper is to show adaptivity may be used for differential-difference equations (DDE) to generate mesh for which ε-uniform convergence is achieved. With solution-adaptive methods, a commonly used technique for determining the grid points is that they equidistribute a positive monitor function of the numerical solution over the domain. For singular perturbation problems the aim is to cluster automatically grid points within a boundary layer and an obvious choice of adaptivity criterion is therefore the solution gradient [8, 10]. Many authors [2, 11] consider upwind scheme applied to the homogeneous version of (1.1) with $\delta = 0$ (one parameter problems) and $b(x) = 0$ on a non-uniform grid formed by equidistribution of the arc-length monitor function $\sqrt{1 + |u'(x)|^2}$. Their analysis and numerical experiments show that the resulting approximation is indeed first-order uniformly convergent.

A description of the contents of the paper is as follows. In Section 2, we establish the maximum principle for the differential operator, stability result and some a priori estimates on the solution and its derivatives. Section 3 presents upwind finite difference discretization and generation of the non-uniform grids through equidistribution principle. We obtain a bound for the local truncation error in Section 4 and carry out the stability and the error analysis which leads to the main theoretical result namely the ε-uniform convergence in the maximum norm. Finally, several numerical examples are provided in Section 5 to illustrate the applicability of the present method with maximum point-wise error and the rate of convergence is shown in terms of tables and figures. This paper ends with Section 6 that summarizes the main conclusions.

Through out this paper C will denote the generic positive constant independent of the perturbation parameter ε and N (the dimension of the discrete problem), the mesh points x_i, which can take different values at different places, even in the same argument. Here $\|\cdot\|$ denotes the supremum norm over $\overline{\Omega}$.

2. Continuous problem

Without loss of generality, we will assume $a(x) > 0$. If $\delta \equiv 0$, then the BVP (1.1) reduces to an ordinary differential equation (ODE) with boundary layer at $x = 0$. In this case, the outer solution

$$u_\varepsilon(x) = \lambda \exp \left[\int_x^1 \frac{b(t)}{a(t)} dt \right] + \mathcal{O}(\varepsilon), \quad \text{as } \varepsilon \to 0,$$

which converges uniformly in x with the solution of (1.1) on $0 \le x_0 \le x \le 1$. In order to find the solution in the layer region, one can follow the standard procedure of singular perturbation analysis by introducing a new variable $\bar{x} = x/\varepsilon$, which yields a solution

$$\bar{u}_\varepsilon(\bar{x}) = \Gamma + (\gamma(0) - \Gamma)e^{-a(0)\bar{x}} + \mathcal{O}(\varepsilon),$$

where $\Gamma = \lambda \exp \left[\int_0^1 (b(t)/a(t)) dt \right]$ in the region $0 < \bar{x} < \infty$ as $\varepsilon \to 0$.

For $\delta = \kappa \varepsilon > 0$, where κ is sufficiently small, we follow the same technique as done in [5, 6]. To tackle the delay term, we will expand the delay argument through Taylor's series expansion assuming sufficient smoothness condition on the solution of (1.1) so that the BVP (1.1) reduces to a standard singular perturbation problem. Here, in this paper, we will focus on this particular case. But for large κ, there may be oscillations in the solution which grow exponentially. The WKB (Wentzel, Kramers and Brillouin) method is developed in [7] to solve such kind of problems and is not discussed in this paper. Now, expanding the shifted term, we obtain

$$u_\varepsilon'(x - \delta) = u_\varepsilon'(x) - \delta u_\varepsilon''(x) + \cdots, \quad \text{as } \varepsilon \to 0. \tag{2.1}$$

Using the first two terms of the expansion (2.1) in the differential equation given by (1.1), we have the following BVP:

$$\begin{cases} L_\varepsilon u(x) \equiv -(\varepsilon - \delta a(x))u''(x) - a(x)u'(x) + b(x)u(x) = f(x), \quad x \in \Omega = (0, 1), \\ u(x) = \gamma(x), \quad -\delta \le x \le 0, \\ u(1) = \lambda. \end{cases} \tag{2.2}$$

It is worthwhile to mention that the BVP (2.2) is the approximate differential equation which differ from the original equation (1.1) by a term which is of $\mathcal{O}(\varepsilon^2)$. Since (2.2) is an approximation of (1.1), so we have used only $u(x)$ as a different notation for $u_\varepsilon(x)$. For convenience, we have taken $\gamma(x)$ as a constant (see [5, 6]). Here, we assume that $\alpha^* \ge a(x) \ge \alpha > 0$ and $(\varepsilon - \delta a(x)) > 0, \forall x \in \overline{\Omega}$. Under these assumptions, the problem (2.2) has a unique solution and it exhibits layer behavior on the left side of the domain at $x = 0$. The layer behavior will remain for sufficiently small non zero values of $\delta(\varepsilon)$.

2.1. Properties of the solution and its derivatives

Lemma 2.1 (Maximum Principle). *Let v be a smooth function satisfying $v(0) \ge 0$, $v(1) \ge 0$ and $L_\varepsilon v(x) \ge 0$, $\forall x \in \Omega$. Then $v(x) \ge 0$, $\forall x \in \overline{\Omega}$.*

Proof. Let $x^* \in \overline{\Omega}$ be such that $v(x^*) = \min v(x)$, $x \in \overline{\Omega}$ and assume that $v(x^*) < 0$. Clearly $x^* \notin \{0, 1\}$ and $v'(x^*) = 0$ and $v''(x^*) \geq 0$. Now consider

$$L_\varepsilon v(x^*) \equiv -(\varepsilon - \delta a(x^*))v''(x^*) - a(x^*)v'(x^*) + b(x^*)v(x^*) < 0,$$

which is a contradiction to our assumption. Hence $v(x) \geq 0, \forall x \in \overline{\Omega}$. □

An immediate consequence of the maximum principle is the following stability estimate.

Lemma 2.2. *If u is the solution of the boundary value problem* (2.2)*, then*

$$\|u\| \leq \frac{1}{\beta}\|f\| + \max\{|u(0)|, |\lambda|\}. \tag{2.3}$$

Proof. Let us consider the following barrier function

$$\psi^\pm(x) = \beta^{-1}\|f\| + \max\{|u(0)|, |\lambda|\} \pm u(x).$$

It is easy to show that $\psi^\pm(x)$ is non-negative at $x = 0, 1$. Now from (2.2),

$$L_\varepsilon \psi^\pm(x) = -(\varepsilon - \delta a(x))(\psi^\pm(x))'' - a(x)(\psi^\pm(x))' + b(x)\psi^\pm(x)$$

$$= b(x)\left[\beta^{-1}\|f\| + \max\{|u(0)|, |\lambda|\}\right] \pm L_\varepsilon u(x)$$

$$\geq \left[\|f\| \pm f(x)\right] + b(x)\max\{|u(0)|, |\lambda|\}$$

$$\geq 0.$$

Thus by applying the maximum principle, we conclude that $\psi^\pm(x) \geq 0, \forall x \in \overline{\Omega}$, which is the desired result. □

Lemma 2.3. *The derivatives $u^{(k)}$ of the solution u of* (2.2) *satisfy the following bound*

$$\|u^{(k)}\| \leq C(\varepsilon + \delta\alpha)^{-k}, \quad k = 1, 2, 3, \tag{2.4}$$

where C depends on $\|a\|$, $\|a'\|$, $\|b\|$, $\|b'\|$ and on the boundary conditions.

Proof. Define a neighborhood $R_x = (r, r + \varepsilon + \delta\alpha)$, where r is a positive constant to be chosen in such a way that for any $x \in \Omega$, $R_x \subset \Omega$. Now applying the mean value theorem, we can find a point $\xi \in R_x$ for which

$$u'(\xi) = \frac{u(r + (\varepsilon + \delta\alpha)) - u(r)}{\varepsilon + \delta\alpha},$$

and hence,

$$|(\varepsilon + \delta\alpha)u'(\xi)| \leq 2\|u\|. \tag{2.5}$$

By integrating the differential equation (2.2) from ξ to x, we obtain

$$(\varepsilon + \delta\alpha)|u'(x)| \leq (\varepsilon + \delta\alpha)|u'(\xi)| + |x - \xi|(\|f\| + \|b\|\|u\|) + \int_\xi^x |a(t)u'(t)| dt. \quad (2.6)$$

We know that

$$\int_\xi^x |a(t)u'(t)| dt \leq 2(\|a\| + \|a'\|)\|u\|. \quad (2.7)$$

Substituting (2.5) and (2.7) in (2.6), we have

$$(\varepsilon + \delta\alpha)|u'(x)| \leq \left[2(\|a\| + \|a'\|) + 2 + \|b\| |x - \xi| \right] \|u\| + |x - \xi| \|f\|. \quad (2.8)$$

From which, we obtain that

$$\|u'\| \leq C (\varepsilon + \delta\alpha)^{-1},$$

where $C = \|f\| + (2 + 2(\|a\| + \|a'\|) + \|b\|)(\beta^{-1}\|f\| + \max\{|u(0)| + |\lambda|\})$ which is independent of ε and δ. Similarly, from (2.2), we have

$$(\varepsilon - \delta a)u'' = bu - au' - f \quad \text{and} \quad \left((\varepsilon - \delta a)u''\right)' = (bu - au' - f)',$$

from which we can obtain successively the required bounds on the second and third derivatives. $\quad\square$

Remark 2.1. The derivatives of $u(x)$, $x \in \overline{\Omega}$, satisfy the following pointwise sharper bounds

$$|u^k(x)| \leq C (\varepsilon + \delta\alpha)^{-k} \exp\left(\frac{-\alpha x}{\varepsilon + \delta\alpha} \right), \quad \text{for } k = 1, 2, 3. \quad (2.9)$$

Proof. Following the technique of [3] for one parameter problem, we can get the desired result. $\quad\square$

3. Discrete problem

3.1. The difference scheme

Consider difference approximations of (2.2) on a non-uniform mesh

$$\Omega_N = \{0 = x_0 < x_1 < x_2 < \cdots < x_{N-1} < x_N = 1\},$$

and denote $h_j = x_j - x_{j-1}$. Without loss of generality, we will assume that N is even. Given a mesh function Z_j, we define the following difference operators:

$$D^+ Z_j = \frac{Z_{j+1} - Z_j}{h_{j+1}}, \quad D^- Z_j = \frac{Z_j - Z_{j-1}}{h_j},$$

$$D^+ D^- Z_j = \frac{2}{h_j + h_{j+1}} \left(\frac{Z_{j+1} - Z_j}{h_{j+1}} - \frac{Z_j - Z_{j-1}}{h_j} \right).$$

The upwind finite difference discretization of (2.2) takes the form

$$
\begin{cases}
L_\varepsilon^N U_j \equiv -(\varepsilon - \delta a_j)D^+D^-U_j - a_j D^+U_j + b_j U_j = f_j, & 1 \le j \le N-1, \\
U_0 \approx \gamma(0) = \gamma_0, \quad U_N = \lambda,
\end{cases}
\tag{3.1}
$$

where U_j denotes the approximation of $u(x_j)$, $a_j = a(x_j)$ and b_j, f_j are defined in a similar fashion. Eq. (3.1) can be expressed in the following form of system of algebraic equations

$$
\begin{cases}
-r_j^- U_{j-1} + r_j^c U_j - r_j^+ U_{j+1} = f_j, & j = 1, \cdots, N-1, \\
U_0 = \gamma_0, \quad U_N = \lambda,
\end{cases}
\tag{3.2}
$$

where

$$
r_j^- = \frac{2(\varepsilon - \delta a_j)}{h_j(h_j + h_{j+1})}, \quad r_j^c = \frac{2(\varepsilon - \delta a_j)}{h_j h_{j+1}} + \frac{a_j}{h_{j+1}} + b_j,
$$

$$
r_j^+ = \frac{2(\varepsilon - \delta a_j)}{h_{j+1}(h_j + h_{j+1})} + \frac{a_j}{h_{j+1}}.
$$

One can easily see that

$$
r_j^- > 0, \ r_j^+ > 0 \quad \text{and} \quad r_j^c + r_j^- + r_j^+ \ge 0, \quad \text{for } j = 1, \cdots, N-1,
\tag{3.3}
$$

which imply that the stiffness matrix is an M-matrix.

3.2. Grid equidistribution

A commonly-used technique in adaptive grid generation is based on the idea of equidistribution. A grid Ω_N is said to be equidistributed if

$$
\int_{x_{j-1}}^{x_j} M\big(u(s), s\big)\, ds = \int_{x_j}^{x_{j+1}} M\big(u(s), s\big)\, ds, \quad j = 1, \cdots, N-1,
\tag{3.4}
$$

where $M\big(u(x), x\big) > 0$ is called a monitor function. Equivalently, (3.4) can be expressed as

$$
\int_{x_j}^{x_{j+1}} M\big(u(s), s\big)\, ds = \frac{1}{N} \int_0^1 M\big(u(s), s\big)\, ds, \quad j = 1, \cdots, N-1.
\tag{3.5}
$$

The optimal choice of monitor function depends on the problem being solved, the numerical discretization being used, and the norm of the error that is to be minimized. In practice, the monitor function is often based on a simple function of the derivatives of the unknown solution.

For practical purposes, it is common to use monitor functions which are bounded away from zero to maintain a sensible distribution of mesh points throughout the domain. Here, we consider the scaled arc-length monitor function

$$
M\big(u(x), x\big) = \sqrt{1 + (u'(x))^2},
\tag{3.6}
$$

which is bounded below by unity. Recently, it has been shown in [2] that the simple upwind scheme is almost first-order accurate on grids based on equidistribution (3.6) when applied to the class of problems of type (2.2) with $\delta = 0$.

3.2.1. Semi-discrete scheme

To simplify the treatment, we construct the monitor function (3.6) in terms of the exact solution of (2.2). Equidistribution can also be thought of as giving rise to a mapping $x = x(\xi)$ relating a computational coordinate $\xi \in [0,1]$ to the physical coordinate $x \in [0,1]$ defined by

$$\int_0^{x(\xi)} M(u(s),s)\,ds = \xi \int_0^1 M(u(s),s)\,ds = \xi \ell, \tag{3.7}$$

where ℓ is the length of u over $\overline{\Omega}$. Now

$$\frac{dx}{d\xi} = \frac{\ell}{\sqrt{1+(u'(x))^2}} \,.$$

More precisely, we have

$$x_j = \int_0^{\xi_j} \frac{\ell}{\sqrt{1+u'(s)^2}}\,ds, \quad \xi_j = \frac{j}{N}, \quad j = 0,\cdots,N. \tag{3.8}$$

Hence, the mesh size is given by

$$h_j = x_j - x_{j-1} = \int_{\xi_{j-1}}^{\xi_j} \frac{\ell}{\sqrt{1+(u'(s))^2}} \, ds\,. \tag{3.9}$$

3.2.2. Fully-discrete scheme

For practical computation, let U_j be the piecewise linear interpolant of knots $(x_j, u(x_j))$. From equidistribution principle (3.7), we have

$$\left[1+(U')^2\right]dx^2 = (\ell\,d\xi)^2 \,.$$

In other words, we can construct the mesh from (3.4) as the solution of the following nonlinear system of equations:

$$\begin{cases} (x_{j+1}-x_j)^2 + (U_{j+1}-U_j)^2 = (x_j - x_{j-1})^2 + (U_j - U_{j-1})^2, \quad j = 1,\cdots,N-1. \\ x_0 = 0, \quad x_N = 1. \end{cases} \tag{3.10}$$

The system of Eqs. (3.1) and (3.10) are solved simultaneously to obtain the solution U_j and the grids x_j. Note that although (3.1) represents a linear set of equations for U_j when the grid is known, the fact that we require the grid to equidistribute a monitor function based on U_j means that the grid is nonlinearly associated to the solution. So even approximating a linear differential equation requires a nonlinear analysis. This is the main reason for the lack of convergence analysis of adaptive grid methods.

Lemma 3.1. *If the mesh Ω_N is generated by (3.9), then*

- *There are $\mathcal{O}(N)$ grid points inside the boundary layer $(0, x_K)$. Moreover, $h_i \leq C(\varepsilon - \delta\alpha)$ for $i \leq K$.*

- *There are $\mathcal{O}(1)$ grid points inside the transition region (x_K, x_J) where $\mathcal{O}(1)$ is independent of ε, δ and N.*

- *There are $\mathcal{O}(N)$ grid points inside the regular region $(x_J, 1)$ and $h_j \leq CN^{-1}$ for $j \geq J + 1$, where $|u'(x)| = \mathcal{O}(\varepsilon + \delta\alpha)^{-1} \gg 1$ if $x < x_J$ and $|u'(x)| = \mathcal{O}(1)$ if $x > x_J$.*

Proof. Following the method of proof provided in [11] for one parameter problem, we can prove the above results. $\qquad\square$

4. Convergence analysis

4.1. Local truncation error

The local truncation error of the difference scheme (3.1) at the node x_j is given by

$$\tau_j = L_\varepsilon^N U_j - (L_\varepsilon u)(x_j), \tag{4.1}$$

where u and U denote the exact solution of (2.2) and (3.1) respectively.

In order to obtain a bound of the local truncation error, we require the following lemmas.

Lemma 4.1. *For any $\psi \in C^3(\overline{\Omega})$, we have*

$$\left|\left(D^+ - \frac{d}{dx}\right)\psi(x_i)\right| \leq \frac{1}{x_{i+1} - x_i} \int_{x_i}^{x_{i+1}} (x_{i+1} - s)\psi''(s)ds,$$

$$\left|\left(D^+D^- - \frac{d^2}{dx^2}\right)\psi(x_i)\right| \leq \frac{1}{x_{i+1} - x_{i-1}}\left[\frac{1}{h_{i+1}} \int_{x_i}^{x_{i+1}} (x_{i+1} - s)^2\psi'''(s)ds \right.$$

$$\left. - \frac{1}{h_i} \int_{x_{i-1}}^{x_i} (s - x_{i-1})^2\psi'''(s)ds\right].$$

Proof. One can find the complete proof of this lemma in Lemma 4.1 of [9]. $\qquad\square$

Lemma 4.2. *The truncation error can be bounded as below*

$$|\tau_j| \leq \frac{C}{(\varepsilon + \delta\alpha)N} \exp\left(\frac{-\alpha x_j}{\varepsilon + \delta\alpha}\right). \tag{4.2}$$

Proof. Using Taylor series expansion and Lemma 4.1, the truncation error (4.1) can be expressed as

$$
\tau_j = \frac{-(\varepsilon - \delta a_j)}{h_j + h_{j+1}} \left[\frac{1}{h_{j+1}} \int_{x_j}^{x_{j+1}} (s - x_{j+1})^2 u'''(s) ds \right.
$$
$$
\left. - \frac{1}{h_j} \int_{x_{j-1}}^{x_j} (s - x_{j-1})^2 u'''(s) ds \right] + \frac{a_j}{h_{j+1}} \int_{x_j}^{x_{j+1}} (s - x_{j+1}) u''(s) ds, \qquad (4.3)
$$

from which we obtain the bound

$$
|\tau_j| < (\varepsilon + \delta \alpha) \int_{x_{j-1}}^{x_{j+1}} |u'''(s)| ds + C \int_{x_{j-1}}^{x_{j+1}} |u''(s)| ds. \qquad (4.4)
$$

Using the bound of the derivative of the continuous solution (2.4) in the first term, the above expression can be written as

$$
|\tau_j| \le C \int_{x_{j-1}}^{x_{j+1}} |u''(s)| ds. \qquad (4.5)
$$

From (3.8), we have

$$
|\tau_j| \le C \ell \int_{\xi_{j-1}}^{\xi_{j+1}} \frac{|u''(x)|}{\sqrt{1 + u'(x)^2}} d\xi
$$
$$
\le \frac{C}{\varepsilon + \delta \alpha} \int_{\xi_{j-1}}^{\xi_{j+1}} \frac{|u'(x)|}{\sqrt{1 + u'(x)^2}} d\xi. \qquad (4.6)
$$

From Lemma 3.1, we know $|u'(x)| = \mathcal{O}(\varepsilon + \delta \alpha)^{-1}$. Again using the bound of the solution (2.9) and the proof provided in [11], we have

$$
\frac{C_1}{\varepsilon + \delta \alpha} \exp\left(\frac{-\alpha^* x}{\varepsilon + \delta \alpha} \right) \le u'(x) \le \frac{C_2}{\varepsilon + \delta \alpha} \exp\left(\frac{-\alpha x}{\varepsilon + \delta \alpha} \right).
$$

Now using these bounds in (4.6), we have

$$
|\tau_j| \le \frac{C}{(\varepsilon + \delta \alpha)} \int_{\xi_{j-1}}^{\xi_{j+1}} \frac{\frac{C_2}{\varepsilon + \delta \alpha} \exp\left(\frac{-\alpha x}{\varepsilon + \delta \alpha} \right)}{\sqrt{1 + (\frac{C_1}{\varepsilon + \delta \alpha})^2 \exp\left(\frac{-2\alpha x}{\varepsilon + \delta \alpha} \right)}} d\xi
$$
$$
\le \frac{C}{N(\varepsilon + \delta \alpha)} \frac{\frac{C_2}{\varepsilon + \delta \alpha} \exp\left(\frac{-\alpha x_j}{\varepsilon + \delta \alpha} \right)}{\sqrt{1 + (\frac{C_1}{\varepsilon + \delta \alpha})^2 \exp\left(\frac{-2\alpha x_j}{\varepsilon + \delta \alpha} \right)}}
$$
$$
\le R_j \exp\left(\frac{-\omega x_j}{\varepsilon + \delta \alpha} \right), \qquad (4.7)
$$

where $0 < \omega < 1$ is independent of ε, N and

$$R_j = \frac{C}{N(\varepsilon + \delta \alpha)} \frac{(C_2/(\varepsilon + \delta \alpha)) \exp\left(-(\alpha - \omega)x_j/(\varepsilon + \delta \alpha)\right)}{\sqrt{1 + (C_1/\varepsilon + \delta \alpha)^2 \exp\left(-2\alpha x_j/(\varepsilon + \delta \alpha)\right)}}.$$

Let us denote

$$y_j = \frac{C}{\varepsilon + \delta \alpha} \exp\left(-\alpha x_j/(\varepsilon + \delta \alpha)\right), \quad g(y) = \frac{y}{\sqrt{1 + y^2}},$$

which is an increasing function in $[0, y^*]$, where $y^* = \sqrt{(1 - \omega)/\omega}$. since $\omega = \mathcal{O}(1)$, we have $y^* = \mathcal{O}(\omega)$ and hence $g(y^*) = \mathcal{O}(1)$. So we can write

$$R_j \leq \frac{C}{N(\varepsilon + \delta \alpha)} g(y_j) \leq \frac{C}{N(\varepsilon + \delta \alpha)} g(y^*) \leq \frac{C}{N(\varepsilon + \delta \alpha)}.$$

Hence,

$$|\tau_j| \leq \frac{C}{(\varepsilon + \delta \alpha)N} \exp\left(\frac{-\alpha x_j}{\varepsilon + \delta \alpha}\right),$$

which is the desired result. $\square$

4.2. Bound on maximum point-wise error

Before deriving the error estimate for the numerical solution of (3.1), we provide here some lemmas which are the prerequisites for the main result.

Lemma 4.3 (Discrete maximum principle)**.** *The system $L_\varepsilon^N V_j = F_j$ with V_0 and V_N specified has a unique solution. If $L_\varepsilon^N V_j < L_\varepsilon^N Z_j$, for $1 \leq j \leq N - 1$ with $V_0 < Z_0$ and $V_N < Z_N$, then $V_j < Z_j$, for $1 \leq j \leq N$.*

Proof. From (3.3), it is clear that the matrix associated with L_ε^N is an irreducible M-matrix and therefore has a positive inverse and hence, the result follows. $\square$

Lemma 4.4. *We define a mesh function S_j by*

$$S_0 = 1, \quad S_j = \prod_{k=1}^{j} \left(1 + \frac{\alpha h_k}{\varepsilon + \delta \alpha}\right)^{-1}, \quad j = 1, \cdots, N. \tag{4.8}$$

Then, for $j = 1, 2, \cdots, N - 1$, there exists a constant C such that

$$L^N S_j \geq \frac{C}{\max\{\varepsilon + \delta \alpha, h_{j+1}\}} S_j. \tag{4.9}$$

Proof. We have

$$\frac{S_j - S_{j-1}}{h_j} = -\frac{\alpha}{\varepsilon + \delta\alpha} S_j .$$

Using the above result yields

$$
\begin{aligned}
L^N S_j &= -\frac{2(\varepsilon - \delta a_j)}{h_j + h_{j+1}} \left[\frac{S_{j+1} - S_j}{h_{j+1}} - \frac{S_j - S_{j-1}}{h_j} \right] - a_j \left[\frac{S_{j+1} - S_j}{h_{j+1}} \right] + b_j S_j \\
&\geq -\frac{2\alpha(\varepsilon - \delta a_j)h_{j+1}}{(\varepsilon + \delta\alpha)(h_j + h_{j+1})} \left[\frac{S_j - S_{j+1}}{h_{j+1}} \right] + \frac{\alpha a_j}{\varepsilon + \delta\alpha} S_{j+1} \\
&\geq \left(\frac{\alpha}{\varepsilon + \delta\alpha + \alpha h_{j+1}} \right) \left[a_j - \frac{2\alpha(\varepsilon - \delta a_j)h_{j+1}}{(\varepsilon + \delta\alpha)(h_j + h_{j+1})} \right] S_j \\
&\geq \frac{C}{\max\{\varepsilon + \delta\alpha, h_{j+1}\}} S_j .
\end{aligned}
$$

This completes the proof of the lemma. □

Remark 4.1. The function S_j is the piecewise $(0,1)$-Padé approximation of $\exp\left(\frac{-\alpha x_j}{\varepsilon + \delta\alpha}\right)$.

In the following lemma, we provide a two-sided bound for S_j, which will be used later.

Lemma 4.5. *The grid function S_j defined in* (4.8) *satisfies*

$$\exp\left(\frac{-\alpha x_j}{\varepsilon + \delta\alpha}\right) < S_j < C \exp\left(\frac{-\alpha x_j}{\varepsilon + \delta\alpha}\right), \quad j = 1, \cdots, N-1. \tag{4.10}$$

Proof. We can express the node x_j as $x_j = \sum_{k=1}^{j} h_k$. Therefore,

$$\exp\left(-\frac{\alpha x_j}{\varepsilon + \delta\alpha}\right) = \exp\left(\sum_{k=1}^{j} \frac{-\alpha h_k}{\varepsilon + \delta\alpha}\right) = \prod_{k=1}^{j} \exp\left(-\frac{\alpha h_k}{\varepsilon + \delta\alpha}\right).$$

For any real value of $\theta > 0$, we have $\exp(-\theta) < (1 + \theta)^{-1}$. Thus, the above expression becomes

$$\exp\left(-\frac{\alpha x_j}{\varepsilon + \delta\alpha}\right) = \prod_{k=1}^{j} \left(1 + \frac{\alpha h_k}{\varepsilon + \delta\alpha}\right)^{-1} < S_j.$$

Now we have to find the upper bound for S_j. Now from (3.9), we have

$$h_j = \int_{\xi_{j-1}}^{\xi_j} \frac{\ell}{\sqrt{1 + (u'(x))^2}} ds$$

We know $\sqrt{1 + (u'(x))^2} \geq u'(x)$ and integrating over the positive integral (ξ_{j-1}, ξ_j), we obtain

$$h_j \leq \int_{\xi_{j-1}}^{\xi_j} \frac{\ell}{u'(x_j)} ds \quad \text{for some } x_j \in (\xi_{j-1}, \xi_j)$$

$$\leq \frac{\ell}{Nu'(x_j)} \quad (\because \text{ using (3.8) where } \xi_j = j/N).$$

Now using the bound

$$|u'(x_j)| \leq C(\varepsilon + \delta\alpha)^{-1} \exp\left(\frac{-\alpha x_j}{\varepsilon + \delta\alpha}\right)$$

in the above inequality, we have

$$h_j \leq \frac{(\varepsilon + \delta\alpha)\ell}{\alpha N} \exp\left(\frac{\alpha x_j}{\varepsilon + \delta\alpha}\right). \tag{4.11}$$

Observe that

$$\ln\left[\prod_{k=1}^{j}\left(1 + \frac{\alpha h_k}{\varepsilon + \delta\alpha}\right)\right] \geq \sum_{k=1}^{j}\left[\frac{\alpha h_k}{\varepsilon + \delta\alpha} - \frac{1}{2}\left(\frac{\alpha h_k}{\varepsilon + \delta\alpha}\right)^2\right]$$

$$\geq \frac{\alpha x_j}{\varepsilon + \delta\alpha} - \frac{1}{2}\sum_{k=1}^{j}\left(\frac{\alpha h_k}{\varepsilon + \delta\alpha}\right)^2. \tag{4.12}$$

Also, we have

$$\sum_{j=1}^{K}\left(\frac{\alpha h_j}{\varepsilon + \delta\alpha}\right)^2 = \left(\frac{\alpha}{\varepsilon + \delta\alpha}\right)^2 \sum_{j=1}^{K} h_j \times h_j.$$

Now for some $\tilde{x}$ in the layer region, *i.e,* $\tilde{x} \in (0, x_K)$, using (3.8) for first h_j *i.e,* $h_j \leq CN^{-1}$ and (4.11) for the second h_j, we can obtain that

$$\sum_{j=1}^{K}\left(\frac{\alpha h_j}{\varepsilon + \delta\alpha}\right)^2 \leq C(\varepsilon + \delta\alpha)^{-1}N^{-1}\sum_{k=1}^{j}\exp\left(\frac{\alpha h_k}{\varepsilon + \delta\alpha}\right)$$

$$\leq C(\varepsilon + \delta\alpha)^{-1}N^{-1}\int_{0}^{\tilde{x}}\exp\left(\frac{\alpha s}{\varepsilon + \delta\alpha}\right)ds$$

$$\leq CN^{-1}\left[\exp\left(\frac{\alpha\tilde{x}}{\varepsilon + \delta\alpha}\right) - 1\right]$$

$$\leq C.$$

Then, from (4.8) and (4.12), we obtain

$$\prod_{k=1}^{j}\left(1 + \frac{\alpha h_k}{\varepsilon + \delta\alpha}\right)^{-1} \leq C\exp\left(\frac{-\alpha x_j}{\varepsilon + \delta\alpha}\right),$$

and hence

$$S_j \leq C \exp\left(\frac{-\alpha x_j}{\varepsilon + \delta\alpha}\right).$$

This completes the proof. □

The main result of this paper, namely the ε-uniform convergence, is given in the following theorem.

Theorem 4.1. *Let $u(x)$ and U_j be respectively the exact solution of (2.2) and the discrete solution of (3.1) on the grids defined by (3.9). Then, there exists a constant C, independent of N, ε and δ such that*

$$\max_{0 \leq j \leq N} |u(x_j) - U_j| \leq CN^{-1}, \qquad j = 0, \cdots, N. \tag{4.13}$$

Proof. We already know from (4.2) that the bound of the truncation error is given by

$$|\tau_j| \leq \frac{C}{(\varepsilon + \delta\alpha)N} \exp\left(\frac{-\alpha x_j}{\varepsilon + \delta\alpha}\right).$$

Let us apply the discrete maximum principle to the barrier function W_j defined by

$$W_j = CN^{-1}(1 + S_j), \quad j = 0, \cdots, N.$$

The truncation error τ_j and the nodal error e_j are related by $L_\varepsilon^N e_j = \tau_j$. Using (4.8), we have for $j = 1, \cdots, N-1$,

$$\begin{aligned}
L_\varepsilon^N e_j = \tau_j &\leq \frac{C}{(\varepsilon + \delta\alpha)N} \exp\left(\frac{-\alpha x_j}{\varepsilon + \delta\alpha}\right) \\
&\leq \frac{C}{(\varepsilon + \delta\alpha)N} S_j \\
&\leq \frac{C}{(\varepsilon + \delta\alpha)N} L_\varepsilon^N S_j \\
&\leq L_\varepsilon^N W_j.
\end{aligned}$$

Since $e_0 \leq W_0$ and $e_N \leq W_N$, we conclude that

$$e_j \leq W_j \leq CN^{-1}, \qquad j = 0, \cdots, N.$$

Now the same argument can be repeated with e_j being replaced by $-e_j$, and hence we have

$$|e_j| \leq CN^{-1}, \qquad j = 0, \cdots, N.$$

which is the desired result. □

4.3. Layer on the right side

Now we assume that the convection coefficient $a(x)$ in the differential equation (1.1) is such that $a(x) \leq \tilde{\alpha} < 0$ for $x \in \overline{\Omega}$ where $\tilde{\alpha}$ is a constant. This assumption implies that the boundary layer occurs in the neighborhood of $x = 1$, *i.e.*, on the right side of the interval. We have already established the estimates for the solution of the continuous problem and its derivatives in the case when the solution of the problem (2.2) exhibits a boundary layer at $x = 0$, *i.e.*, at the left side of the interval $[0, 1]$. One can easily obtain similar estimates for the right boundary layer case. But the main difference in this kind of approach is the numerical scheme where we approximate the first-order derivative by the backward finite difference operator in place of the forward finite difference operator as we did in case of left side boundary layer. This is mainly for the stability of the upwind scheme.

Hence the numerical scheme is of the form

$$\begin{cases} L_\varepsilon N U_j \equiv -(\varepsilon - \delta a_j) D^+ D^- U_j + a_j D^- U_j + b_j U_j = f_j, & 1 \leq j \leq N - 1, \\ U_0 = \gamma_0, \quad U_N = \lambda. \end{cases} \tag{4.14}$$

The above equation can be expressed in the form

$$\begin{cases} -r_j^- U_{j-1} + r_j^c U_j - r_j^+ U_{j+1} = f_j, & j = 1, \cdots, N-1, \\ U_0 = \gamma_0, \quad U_N = \lambda, \end{cases} \tag{4.15}$$

where

$$r_j^- = \frac{2(\varepsilon - \delta a_j)}{h_j(h_j + h_{j+1})} + \frac{a_j}{h_j}, \quad r_j^c = \frac{2(\varepsilon - \delta a_j)}{h_j h_{j+1}} + \frac{a_j}{h_j} + b_j, \quad r_j^+ = \frac{2(\varepsilon - \delta a_j)}{h_{j+1}(h_j + h_{j+1})}.$$

One can easily see that the stiffness matrix (4.15) is an irreducible M-matrix.

Here it is significant to observe that we can construct non-uniform mesh as given in (3.10) through the same monitor function defined in (3.6) in the case of right boundary layer without any extra care.

5. Numerical results

In this section to validate the theoretical results, we apply the proposed numerical scheme to several test problems with constant and variable coefficients having left and right boundary layers. For comparison purposes, we use the upwind differences scheme on the piecewise-uniform Shishkin mesh.

5.1. Shishkin mesh for the left boundary layer

The piecewise-uniform Shishkin mesh $\overline{\Omega}_\varepsilon$ is constructed by partitioning the domain $[0, 1]$ into two subdomains $[0, \tau]$ and $[\tau, 1]$. Here τ denotes the transition parameter which determines the point of transition from a fine mesh to the coarse mesh and is defined

as $\tau = \min\{1/2, (\varepsilon - \delta\alpha)\ln N/\beta\}$, where β, α are defined earlier. The definition of τ guarantees the existence of some points inside the layer region. Now we will place $N/2$ numbers of subintervals in each of the subdomains. Hence the Shishkin mesh will be of the form

$$\overline{\Omega}_\varepsilon = \left\{x_i : x_i = 2\tau i/N, \ i \leq N/2; \ x_i = x_{i-1} + 2(1-\tau)/N, \ N/2 < i \leq N\right\}.$$

Note that τ depends on N, if it is chosen independently of N, then the ε-uniform convergence of the upwind scheme can not be guaranteed [3]. Similarly for right boundary layer problems, the corresponding Shishkin mesh can be formed by dividing the domain $[0, 1]$ into two subdomains $[0, 1 - \tau]$ and $[1 - \tau, 1]$.

Example 5.1. Consider the constant coefficient problem

$$\begin{cases} -\varepsilon u''(x) - u'(x - \delta) + u(x) = 0, & x \in \Omega, \\ u(x) = 1, & -\delta \leq x \leq 0, \\ u(1) = 1. \end{cases} \tag{5.1}$$

The approximate differential equation to Example 5.1 is of the form

$$\begin{cases} -(\varepsilon - \delta)u''(x) - u'(x) + u(x) = 0, & x \in \Omega, \\ u(x) \approx u(0) = 1, & -\delta \leq x \leq 0, \\ u(1) = 1. \end{cases} \tag{5.2}$$

The exact solution of (5.2) is given by

$$u(x) = C_1 \exp(m_1 x) + C_2 \exp(m_2 x),$$

where

$$m_{1,2} = \frac{-1 \mp \sqrt{1 + 4(\varepsilon - \delta)}}{2(\varepsilon - \delta)}, \quad C_1 = \frac{1 - \exp(m_2)}{\exp(m_1) - \exp(m_2)}, \quad C_2 = \frac{\exp(m_1) - 1}{\exp(m_1) - \exp(m_2)}.$$

This solution has a boundary layer at $x = 0$.

Example 5.2. Consider the following variable coefficient delay differential equation

$$\begin{cases} -\varepsilon u''(x) - \exp(-x)u'(x - \delta) + xu(x) = 0, & x \in \Omega, \\ u(x) = 1, & -\delta \leq x \leq 0, \\ u(1) = 1. \end{cases}$$

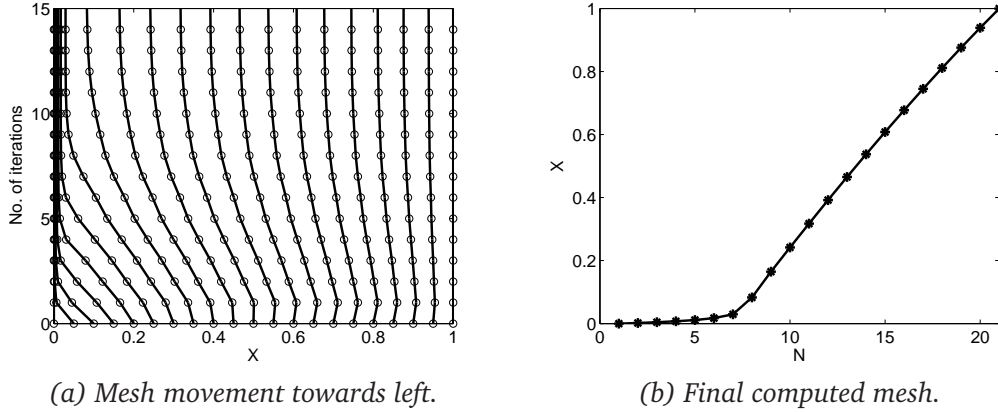Here the boundary layer occurs at $x = 0$ and the exact solution is not known.

(a) Mesh movement towards left.   (b) Final computed mesh.

Figure 1: Movement of the mesh points towards left for Example 5.1 for $\varepsilon = 10^{-2}$, $\delta = 10^{-8}$ and No. of subintervals $N = 20$.

Example 5.3. Consider the constant coefficient problem with right hand side boundary layer

$$\begin{cases} \varepsilon u''(x) - u'(x - \delta) - u(x) = 0, & x \in \Omega, \\ u(x) = 1, & -\delta \le x \le 0, \\ u(1) = -1. \end{cases}$$

The above problem has a boundary layer near $x = 1$. The exact solution of the approximated BVP is given by

$$u(x) = C_1 \exp(m_1 x) - C_2 \exp(m_2 x),$$

where

$$m_{1,2} = \frac{1 \mp \sqrt{1 + 4(\varepsilon + \delta)}}{2(\varepsilon + \delta)}, \quad C_1 = \frac{1 + \exp(m_2)}{\exp(m_2) - \exp(m_1)}, \quad C_2 = \frac{\exp(m_1) + 1}{\exp(m_2) - \exp(m_1)}.$$

Example 5.4. The final example is the non-constant coefficient problem

$$\begin{cases} \varepsilon u''(x) - (1 + x)u'(x - \delta) - \exp(-x)u(x) = 1, & x \in \Omega, \\ u(x) = 1, & -\delta \le x \le 0, \\ u(1) = -1. \end{cases}$$

In this BVP, the boundary layer is at $x = 1$ and the exact solution is not known.

Fig. 1(a) represents the movement of mesh after each iteration and Fig. 1(b) the final computed mesh corresponding to the solution of Example 5.1. It is prominent from these figures that the mesh starts to move toward the boundary layer and clusters as many points required for the layer region. So this kind of approach has the advantage that without any prior knowledge of the location of the boundary layer, we are able to generate some points
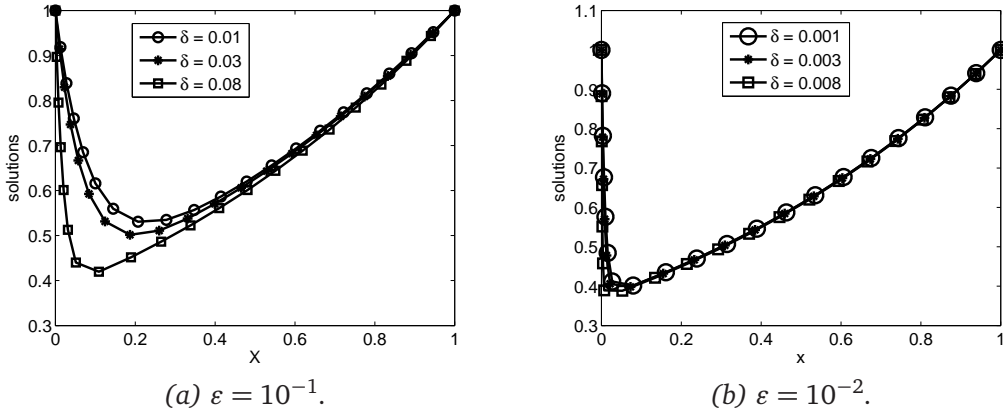
(a) $\varepsilon = 10^{-1}$.   *(b)* $\varepsilon = 10^{-2}$.

Figure 2: Effect of δ on the solution of Example 5.1 for $N = 20$ with different values of ε.
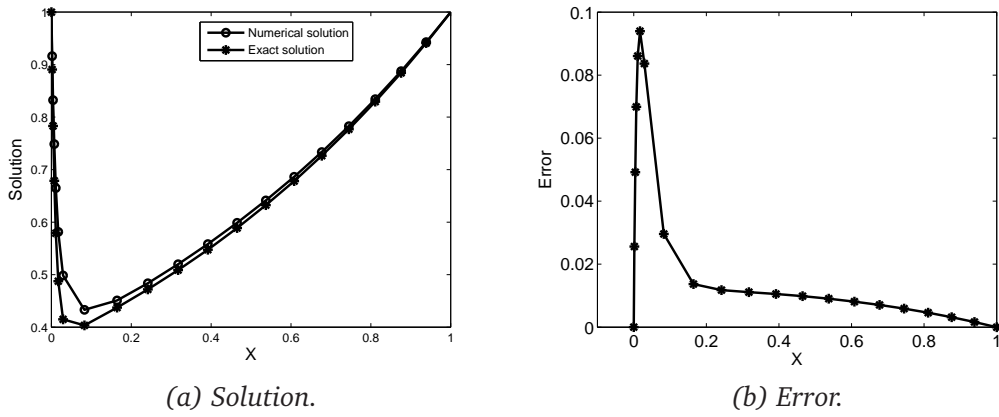

(a) Solution.   *(b) Error.*

Figure 3: Numerical solution with exact solution and the corresponding error of Example 5.1 for $\varepsilon = 10^{-2}$, $\delta = 10^{-8}$ and $N = 20$.

inside the layer region. In Figs. 2(a) and 2(b), we present the effect of δ on the solution of Example 5.1 and finally Figs. 3(a) and 3(b) represent the corresponding solution and the error. Also we have plotted similar graphs in the case when the boundary layer is located at right side of the domain *i.e,* for Example 5.3. In Fig. 4(a), we represent the movement of the mesh towards right. Moreover, Fig. 5 represents the effect of δ on the right boundary layer whereas Fig. 6 represents the computed solution along with the error.

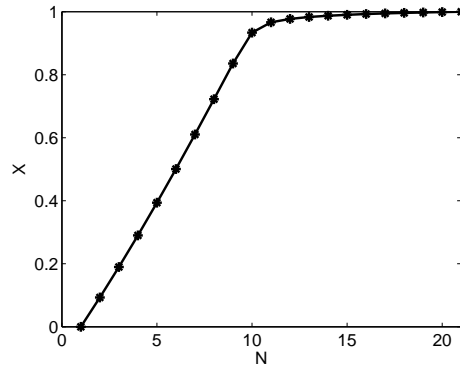Further, for any value of N, the maximum pointwise errors E_ε^N are calculated by

$$E_\varepsilon^N = \|u(x_j) - U_j\|,$$

where u is the exact solution and U_j is the numerical solution. We use the double mesh method to compute the rate of convergence as

$$p^N = \log_2 \left(\frac{E_\varepsilon^N}{E_\varepsilon^{2N}} \right).$$
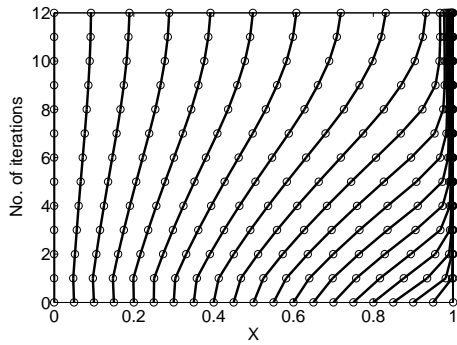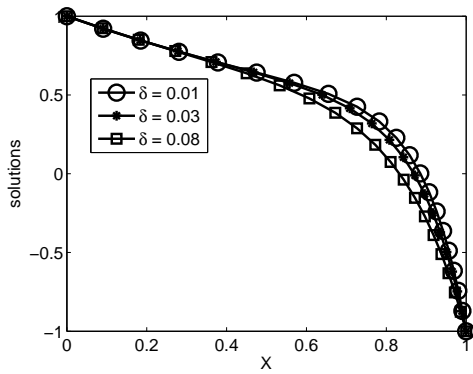
(a) Mesh movement towards right.   (b) Final computed mesh.

Figure 4: Movement of the mesh points towards right for Example 5.3 for $\varepsilon = 10^{-2}$, $\delta = 10^{-8}$ and $N = 20$.
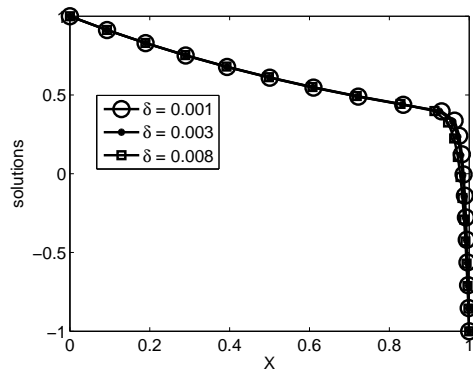
(a) $\varepsilon = 10^{-1}$.   (b) $\varepsilon = 10^{-2}$.

Figure 5: Effect of δ on the solution of Example 5.3 for $N = 20$ with different values of ε.

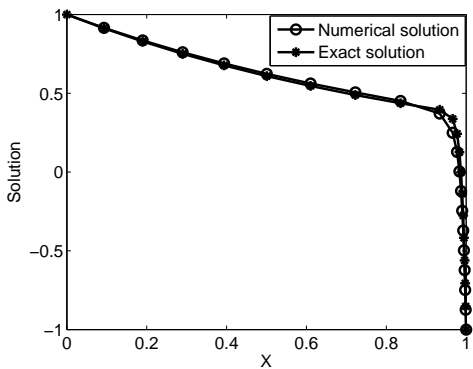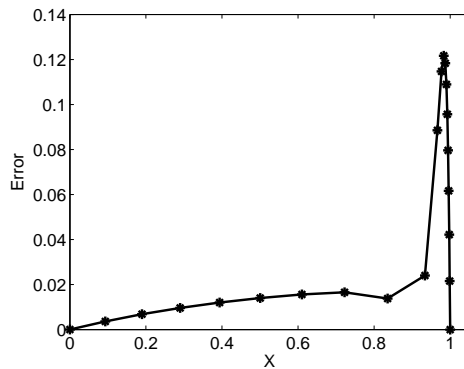(a) Solution.   (b) Error.

Figure 6: Numerical solution with exact solution and the corresponding error of Example 5.3 for $\varepsilon = 10^{-2}$, $\delta = 10^{-8}$ and $N = 20$.

Table 1: Maximum point-wise errors E_ε^N and the rate of convergence p^N generated for $\delta = 10^{-12}$ of Example 5.1.

ε	Number of intervals N						
	16	32	64	128	256	512	1024
1	3.0659e-3	1.5556e-3	7.8448e-4	3.9372e-4	1.9723e-4	9.8711e-5	4.9379e-5
	0.9788	0.9877	0.9946	0.9973	0.9986	0.9993	
10^{-2}	1.0806e-1	6.5947e-2	3.8353e-2	2.1065e-2	1.1113e-2	5.7156e-3	2.8937e-3
	0.7125	0.7820	0.8645	0.9226	0.9593	0.9820	
10^{-4}	1.2463e-1	8.4308e-2	4.9399e-2	2.8705e-2	1.6724e-2	9.2803e-3	5.1829e-3
	0.5640	0.7712	0.7831	0.7794	0.8497	0.8404	
10^{-8}	1.2485e-1	8.5355e-2	4.9662e-2	2.8857e-2	1.6891e-2	9.4111e-3	5.3383e-3
	0.5486	0.7813	0.7832	0.7727	0.8438	0.8180	
10^{-10}	1.2485e-1	8.5353e-2	4.9660e-2	2.8861e-2	1.6891e-2	9.4096e-3	5.3377e-3
	0.5487	0.7814	0.7830	0.7728	0.8441	0.8179	

Table 2: Maximum point-wise errors G_ε^N and the rate of convergence q^N generated for $\delta = 10^{-12}$ of Example 5.2.

ε	Number of intervals N						
	16	32	64	128	256	512	1024
1	1.1255e-3	5.5409e-4	2.7353e-4	1.3420e-4	6.4849e-5	3.0251e-5	1.2971e-5
	1.0224	1.0184	1.0273	1.0492	1.1001	1.2217	
10^{-2}	1.3551e-1	8.0474e-2	4.4173e-2	2.2810e-2	1.0904e-2	4.4767e-3	1.8415e-3
	0.7518	0.8654	0.9535	1.0648	1.2843	1.2816	
10^{-4}	8.2523e-2	5.7914e-2	3.9768e-2	2.3760e-2	1.3183e-2	7.4077e-3	3.4080e-3
	0.5109	0.5423	0.7431	0.8499	0.8316	1.1201	
10^{-8}	6.7670e-2	5.5369e-2	3.6724e-2	2.4701e-2	1.4268e-2	6.9121e-3	3.7731e-3
	0.2894	0.5924	0.5722	0.7918	1.0456	0.8734	
10^{-10}	8.1067e-2	5.6218e-2	3.9495e-2	2.2684e-2	1.2954e-2	6.0157e-3	2.4715e-3
	0.5281	0.5094	0.8000	0.8083	1.1066	1.2833	

Table 3: Maximum point-wise errors E_ε^N and the rate of convergence p^N generated for $\delta = 10^{-12}$ of Example 5.3 .

ε	Number of intervals N						
	16	32	64	128	256	512	1024
1	5.6304e-3	2.9283e-3	1.4940e-3	7.5461e-4	3.7920e-4	1.9007e-4	9.5157e-5
	0.9432	0.9709	0.9854	0.9928	0.9964	0.9982	
10^{-2}	1.4267e-1	8.5082e-2	4.7691e-2	2.5498e-2	1.3224e-2	6.7357e-3	3.6940e-3
	0.7457	0.8351	0.9033	0.9473	0.9732	0.8666	
10^{-4}	1.7424e-1	1.0885e-1	6.5746e-2	3.8706e-2	2.2167e-2	1.2374e-2	6.7611e-3
	0.6787	0.7274	0.7643	0.8042	0.8410	0.8720	
10^{-8}	1.7484e-1	1.0929e-1	6.6127e-2	3.9070e-2	2.2929e-2	1.2822e-2	7.1847e-3
	0.6779	0.7248	0.7592	0.7689	0.8385	0.8357	
10^{-10}	1.7461e-1	1.0933e-1	6.6169e-2	3.9106e-2	2.2958e-2	1.2527e-2	7.0556e-3
	0.6755	0.7244	0.7588	0.7684	0.8740	0.8282	

Table 4: Maximum point-wise errors G_ε^N and the rate of convergence q^N generated for $\delta = 10^{-12}$ of Example 5.4.

ε	Number of intervals N						
	16	32	64	128	256	512	1024
1	9.3312e-3	4.9243e-3	2.5101e-3	1.2515e-3	6.0855e-4	2.8368e-4	1.2042e-4
	0.9221	0.9721	1.0041	1.0402	1.1011	1.2362	
10^{-2}	1.0985e-1	6.5425e-2	3.6239e-2	1.7269e-2	6.2503e-3	3.2809e-3	1.7116e-3
	0.7476	0.8523	1.0694	1.4662	0.9298	0.9387	
10^{-4}	5.4976e-2	3.6507e-2	2.7036e-2	1.8143e-2	1.1740e-2	6.6864e-3	3.4611e-3
	0.5906	0.4333	0.5755	0.6280	0.8121	0.9500	
10^{-8}	1.7226e-1	8.9547e-2	3.8862e-2	1.9892e-2	1.0979e-2	6.1047e-3	3.2755e-3
	0.9439	1.2043	0.9662	0.8574	0.8468	0.8982	
10^{-10}	1.5374e-1	7.2108e-2	3.7251e-2	1.7697e-2	1.0527e-2	5.5295e-3	2.1111e-3
	1.0923	0.9529	1.0738	0.7494	0.9289	1.3892	

Table 5: Comparison between computational results for Shishkin mesh and Adaptive mesh with $\delta = 10^{-12}$ for Example 5.2. $\varepsilon = 10^{-4}$.

$\varepsilon = 10^{-4}$	Number of intervals N						
	16	32	64	128	256	512	1024
Shishkin mesh	9.1183e-2	5.3514e-2	3.8978e-2	3.1089e-2	2.6349e-2	2.2549e-2	1.7990e-2
	0.7689	0.4572	0.3263	0.2387	0.2247	0.3259	
Adaptive mesh	8.2523e-2	5.7914e-2	3.9768e-2	2.3760e-2	1.3183e-2	7.4077e-3	3.4080e-3
	0.5109	0.5423	0.7431	0.8499	0.8316	1.1201	

Table 6: Same as Table 5, except with $\varepsilon = 10^{-8}$.

$\varepsilon = 10^{-8}$	Number of intervals N						
	16	32	64	128	256	512	1024
Shishkin mesh	9.1050e-2	4.7252e-2	2.3922e-2	1.1892e-2	5.7837e-3	2.7066e-3	1.1628e-3
	0.9463	0.9820	1.0084	1.0399	1.0955	1.2189	
Adaptive mesh	6.7670e-2	5.5369e-2	3.6724e-2	2.4701e-2	1.4268e-2	6.9121e-3	3.7731e-3
	0.2894	0.5924	0.5722	0.7918	1.0456	0.8734	

In Tables 1 and 3, we present the maximum pointwise error and the corresponding order of convergence for Examples 5.1 and 5.3, respectively.

The exact solutions are not available for Examples 5.2 and 5.4. In order to calculate the maximum point-wise error G_ε^N and the rate of convergence q^N, we use interpolation. Define $\overline{U}^{4096}$ as the piecewise linear interpolation to U^N in Ω_N. Define,

$$G_\varepsilon^N = \max_{x_i \in \overline{\Omega}^N} |U^N - \overline{U}^{4096}| \quad \text{and} \quad q^N = \log_2 \left(\frac{G_\varepsilon^N}{G_\varepsilon^{2N}} \right).$$

The maximum pointwise error and the corresponding order of convergence for the Examples 5.2 and 5.4 are provided in Tables 2 and 4, respectively.
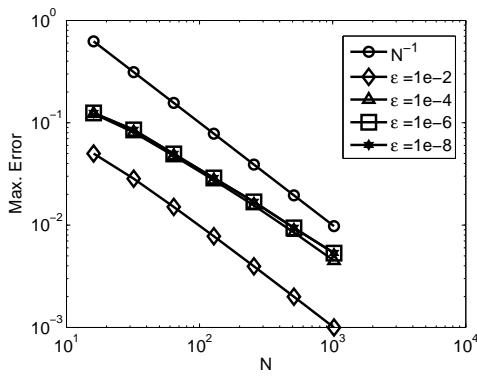
We have also compared the computational results using adaptive mesh to the computational results of the Shishkin mesh which is shown in Tables 5 and 6 for Example 5.2. From

Table 7: Comparison between computational results for Shishkin mesh and Adaptive mesh with $\delta = 10^{-12}$ for Example 5.4. $\varepsilon = 10^{-4}$.
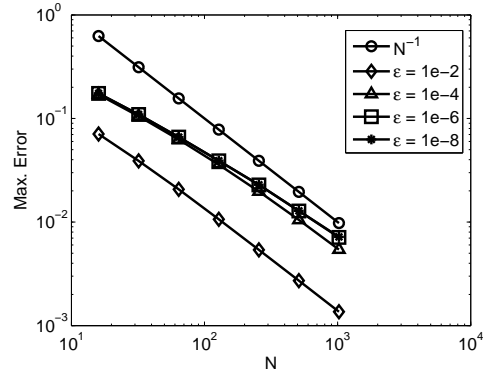
$\varepsilon = 10^{-4}$	Number of intervals N						
	16	32	64	128	256	512	1024
Shishkin	6.5329e-2	3.3874e-2	1.7207e-2	1.5572e-2	1.5174e-2	1.4100e-2	1.1865e-2
mesh	0.9476	0.9772	0.1440	0.0373	0.1060	0.2489	
Adaptive	5.4976e-2	3.6507e-2	2.7036e-2	1.8143e-2	1.1740e-2	6.6864e-3	3.4611e-3
mesh	0.5906	0.4333	0.5755	0.6280	0.8121	0.9500	

Table 8: Same as Table 7, except with $\varepsilon = 10^{-8}$.

$\varepsilon = 10^{-8}$	Number of intervals N						
	16	32	64	128	256	512	1024
Shishkin	6.5499e-2	3.4127e-2	1.7300e-2	8.6037e-3	4.1850e-3	1.9579e-3	8.4012e-4
mesh	0.5906	0.4333	0.5755	0.6280	0.8121	0.9501	
Adaptive	1.7226e-1	8.9547e-2	3.8862e-2	1.9892e-2	1.0979e-2	6.1047e-3	3.2755e-3
mesh	0.9439	1.2043	0.9662	0.8574	0.8468	0.8982	

(a) Example 5.1.   *(b) Example 5.3.*

Figure 7: Loglog plot of the maximum error for different values of ε.

these results, one can observe that adaptive mesh gives comparative results than Shishkin mesh. Similarly the comparison for Example 5.4 is also shown in Tables 7 and 8 in the case of right boundary layer.

In order to visualize the order of convergence, the loglog plot of the maximum error is shown in Figs. 7(a) and 7(b) for Examples 5.1 and 5.3 respectively. From these figures and the numerical results shown in tables, we conclude that the proposed method is ε-uniform convergent of order one.

6. Conclusion

In this article, we proposed a numerical method to solve singularly perturbed delay differential equations of the form (1.1)-(2.2). We applied the upwind finite difference scheme

on a nonuniform mesh which is generated adaptively from equidistribution principle. The equidistribution is done with the help of a positive monitor function which contains the first-derivative of the solution. We carried out the error analysis for the numerical solution which shows the first-order ε-uniform convergence of the proposed method. From the numerical results presented in the previous section, we conclude that the errors converge at the rate of first-order, independent of the small perturbation parameters. Hence if the mesh is generated adaptively, it is possible to obtain approximate solutions that converge uniformly without depending on the small parameters.

References

[1] Y. Chen, *Uniform pointwise convergence for a singularly perturbed problem using arc-length equidistribution*, J. Comput. Appl. Math., 159 (2003), pp. 25–34.

[2] Y. Chen, *Uniform convergence analysis of finite difference approximations for singularly perturbation problems on an adapted grid*, Adv. Comput. Math., 24 (2006), pp. 197–212.

[3] P.A. Farrell, A.F. Hegarty, J.J.H. Miller, E. O'Riordan, and G.I. Shishkin, *Robust Computational Techniques for Boundary Layers*, Chapman & Hall/CRC Press, Boca Raton, FL, 2000.

[4] R.B. Kellogg and A. Tsan, *Analysis of some difference approximations for a singular perturbation problem without turning point*, Math. Comp., 32 (144), (1978), pp. 1025–1039.

[5] C.G. Lange and R.M. Miura, *Singular perturbation analysis of boundary-value problems for differential-difference equations*, SIAM J. Appl. Math., 42 (3), (1982), pp. 502–531.

[6] C.G. Lange and R.M. Miura, *Singular perturbation analysis of boundary-value problems for differential-difference equations. V. small shifts with layer behavior*, SIAM J. Appl. Math., 54 (1), (1994), pp. 249–272.

[7] C.G. Lange and R.M. Miura, *Singular perturbation analysis of boundary-value problems for differential-difference equations. VI. small shifts with rapid oscillations*, SIAM J. Appl. Math., 54 (1), (1994), pp. 273–283.

[8] J. Mackenzie, *Uniform convergence analysis of an upwind finite difference approximation of a convection-diffusion boundary value problem on an adaptive grid*, IMA J. Numer Anal., 19, (1999), pp. 233–249.

[9] J.J.H. Miller, E. O'Riordan, and G.I. Shishkin, *Fitted Numerical Methods for Singular Perturbation Problems*, World Scientific, Singapore, 1996.

[10] Y. Qiu and D.M. Sloan, *Analysis of difference approximations to a singularly perturbed two point boundary value problem on an adaptively generated grid*, J. Comput. Appl. Math., 101, (1999), pp. 1–25.

[11] Y. Qiu, D.M. Sloan, and T. Tang, *Numerical solution of a singularly perturbed two point boundary value problem using equidistribution: analysis of convergence*, J. Comput. Appl. Math., 116, (2000), pp. 121–143.

[12] R.B. Stein, *Some models of neuronal variability*, Biophysical Journal, 7, (1967), pp. 37–68.